Article

Cell Reports

Time-Resolved Fast Mammalian Behavior Reveals the Complexity of Protective Pain Responses

Graphical Abstract

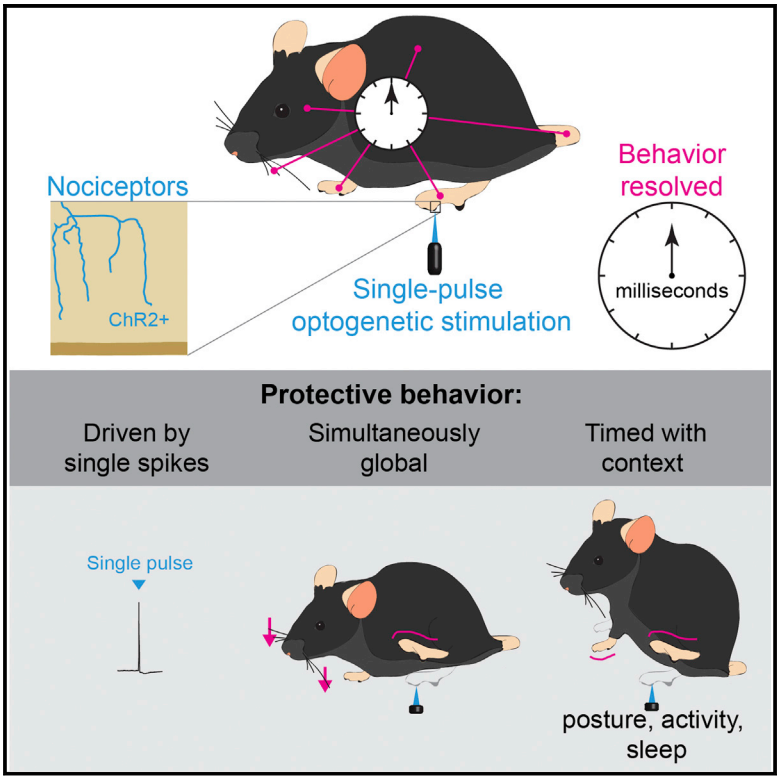

Authors

Liam E. Browne, Alban Latremoliere, Brendan P. Lehnert, ..., David P. Roberson, David D. Ginty, Clifford J. Woolf

Correspondence

liam.browne@ucl.ac.uk (L.E.B.), clifford.woolf@childrens.harvard.edu (C.J.W.)

In Brief

Browne et al. find that the responses evoked by noxious stimuli, when examined at a millisecond resolution, are not fixed, localized, or limited to reflex withdrawal but are instead coordinated globally across the body in a sub-second time frame to alert the animal and limit potential harm.

Highlights

- Protective behavior examined at a millisecond resolution
- A localized single action potential input initiates simultaneous global responses
- Protective behavioral responses are coordinated according to the state of the animal
- A local single action potential volley causes sub-second sleep-wake transitions

Browne et al., 2017, Cell Reports *20*, 89–98
July 5, 2017
http://dx.doi.org/10.1016/j.celrep.2017.06.024

Cell Reports
Article

Time-Resolved Fast Mammalian Behavior Reveals the Complexity of Protective Pain Responses

Liam E. Browne,[1,2,3,7,*] Alban Latremoliere,[1,2] Brendan P. Lehnert,[1,4] Alyssa Grantham,[2] Catherine Ward,[2] Chloe Alexandre,[1,5] Michael Costigan,[1,2,6] Frédéric Michoud,[1,2] David P. Roberson,[1,2] David D. Ginty,[1,4] and Clifford J. Woolf[1,2,*]

[1]Department of Neurobiology, Harvard Medical School, Boston, MA 02115, USA
[2]FM Kirby Neurobiology Center, Boston Children's Hospital, Boston, MA 02115, USA
[3]Wolfson Institute for Biomedical Research, University College London, London WC1E 6BT, UK
[4]Howard Hughes Medical Institute, Chevy Chase, MD 20815-6789, USA
[5]Department of Neurology, Beth Israel Deaconess Medical Center, Boston, MA 02115, USA
[6]Department of Anesthesia, Boston Children's Hospital, Boston, MA 02115, USA
[7]Lead Contact
*Correspondence: liam.browne@ucl.ac.uk (L.E.B.), clifford.woolf@childrens.harvard.edu (C.J.W.)
http://dx.doi.org/10.1016/j.celrep.2017.06.024

SUMMARY

Potentially harmful stimuli are detected at the skin by nociceptor sensory neurons that drive rapid protective withdrawal reflexes and pain. We set out to define, at a millisecond timescale, the relationship between the activity of these sensory neurons and the resultant behavioral output. Brief optogenetic activation of cutaneous nociceptors was found to activate only a single action potential in each fiber. This minimal input was used to determine high-speed behavioral responses in freely behaving mice. The localized stimulus generated widespread dynamic repositioning and alerting sub-second behaviors whose nature and timing depended on the context of the animal and its position, activity, and alertness. Our findings show that the primary response to injurious stimuli is not limited, fixed, or localized, but is dynamic, and that it involves recruitment and gating of multiple circuits distributed throughout the central nervous system at a sub-second timescale to effectively both alert to the presence of danger and minimize risk of harm.

INTRODUCTION

Potentially damaging noxious stimuli activate high-threshold primary afferent neurons, the nociceptors, which include sensory neurons with thinly myelinated (Aδ) or unmyelinated (C) axons (Julius, 2013; Prescott et al., 2014; Woolf, 1983). In a series of seminal studies that represented the first analysis of circuits in the central nervous system, Sir Charles Sherrington showed that cutaneous nociceptors activate spinal reflex arcs to drive the withdrawal of an affected limb from the potential source of harm (Sherrington, 1910). Subsequent work found that each motor pool has distinctive excitatory and inhibitory cutaneous receptive fields to produce a hindlimb movement specific to a precise stimulation site, the "modular" theory of withdrawal reflex organization (Schouenborg and Kalliomäki, 1990; Schouenborg and Weng, 1994). Nociceptive withdrawal reflexes are considered the basic unit of protective pain-related behavior and are presumed to represent one of the simplest polysynaptic relationships between sensory input and motor output (Clarke and Harris, 2004). These protective responses need to be rapid and yet coordinated appropriately. However, the relationship between a purely nociceptive stimulus and the global resultant behavior has not been studied with high temporal resolution.

How do nociceptor inputs initiate rapid behaviors that are most appropriate for dealing with a specific harmful threat to a particular anatomical site, and are these responses localized or widely distributed? How much input is required to trigger a response and to what extent is the behavior maintained by ongoing input from the periphery? Many such questions remain unanswered because behavioral and sensory responses to noxious stimuli are commonly applied and measured over a timescale of seconds, even though the nervous system operates in the millisecond range.

Optogenetics enables specific activation of genetically defined primary afferents in a localized area with high temporal control, but this technology has only been applied with low temporal resolution (Daou et al., 2013; Iyer et al., 2014). Recently, Arcourt et al. (2017) used single-shot optogenetic stimulation to identify an interaction between low-threshold mechanoreceptors and A-fiber nociceptors by examining local sub-second behavioral responses at 240 frames per second. Here we examine the repertoire of behavioral responses on even faster timescales across the whole animal. We mapped the fast, global structure of evoked responses in awake, freely behaving animals by combined single-shot millisecond optogenetic activation of cutaneous nociceptors with millisecond (1-kHz) sampling of behavior (Figure 1A). The relative timings for regional and general responses to a single time-locked input were used to examine the nature and coordination of the behavioral output. We reveal the complexity and diversity with which the nervous system coordinates fast protective behavior across the whole animal, identifying responses that could only be observed at a millisecond

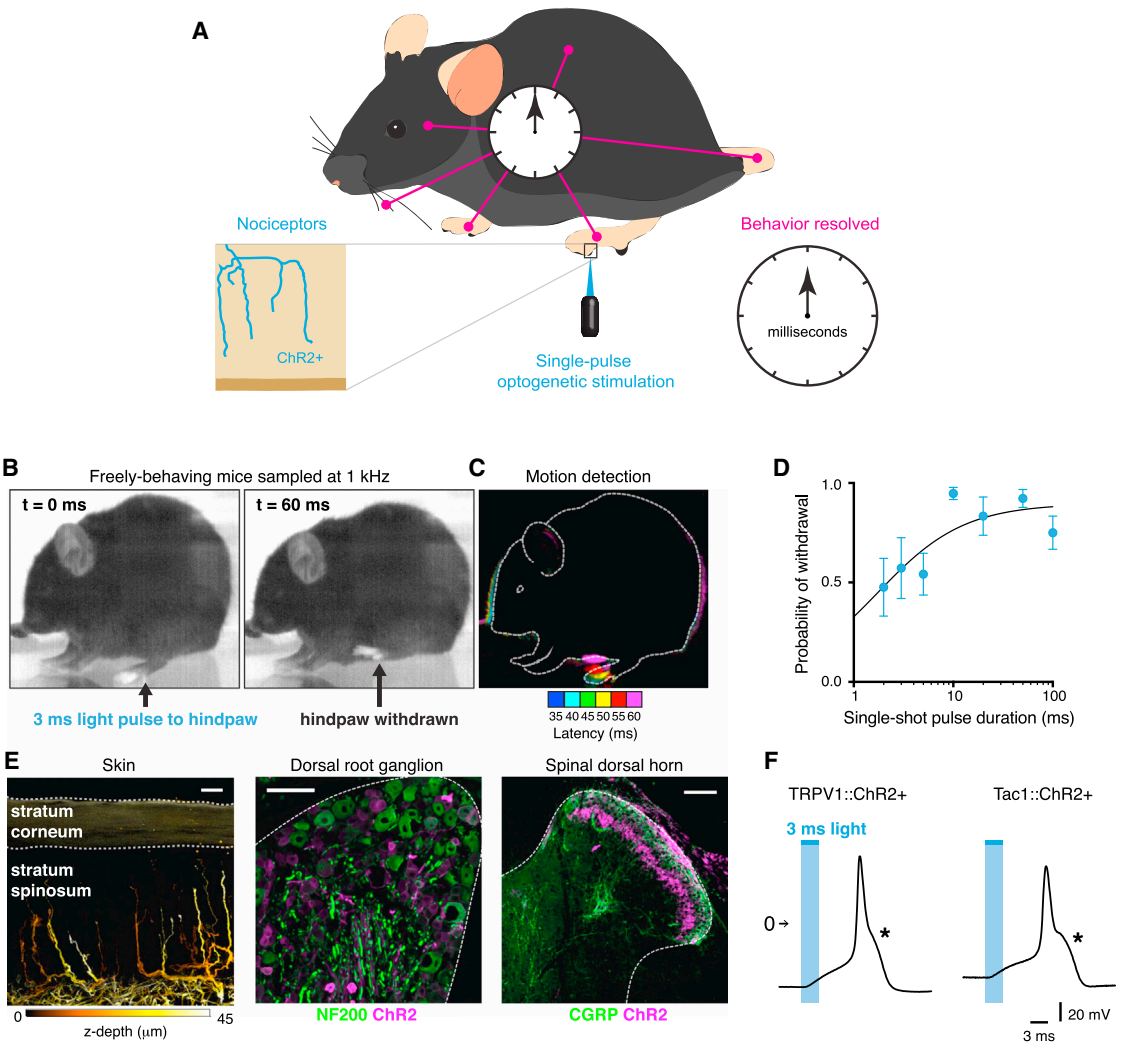

Figure 1. Rapid Protective Behavior Time-Resolved Using Single-Pulse Optogenetic Activation and High-Speed Sampling

(A) Schematic illustrating the strategy used to map the fine-grained evoked behavioral responses with millisecond resolution.

(B) Behavior elicited by a 3-ms light pulse to the hindpaw to monitor the nature, extent, timing, and coordination of limb movements associated with flexion withdrawal using a camera recording at 1,000 frames per second. TRPV1::ChR2 is shown.

(C) Motion detected by comparing the difference in pixel intensity between frames. Each color represents the position of the animal at a point in time. The first motion was detected 35 ms from start of the 3-ms optogenetic stimulus.

(D) Probability of flexion withdrawal depended on pulse duration (four TRPV1::ChR2 mice, six to ten trials each). Data are represented as mean ± SEM.

(E) ChR2 was expressed in nociceptors that innervate the skin and spinal cord, as shown here for TRPV1::ChR2. Scale bars, 20 μm.

(F) Current-clamp recordings of cultured DRG neurons show that a 3-ms pulse of light generates a high-threshold action potential with a pronounced shoulder, as indicated by the asterisks.

timescale. Such an approach may have general utility for studying stimulus-evoked behaviors.

RESULTS

Single-Pulse Optogenetic Activation of Nociceptors Evokes Rapid Protective Behaviors

We expressed the light-activated ion channel ChR2 in two broad classes of cutaneous nociceptor afferents by crossing Cre-dependent ChR2-tdTomato mice (Madisen et al., 2012) with either TRPV1-Cre or Tac1-Cre mice (Basbaum et al., 2009; Cavanaugh et al., 2011; Harris et al., 2014). In the resultant mice, freely behaving on a glass floor, a single pulse of blue light as short as 3 ms to the glabrous hindpaw surface caused hindlimb withdrawal in most trials (Figures 1B–1D). Increasing the duration of the light stimulus increased response probability (Figure 1D). The blue light was delivered as a small 900-μm spot to the hindpaw (~1% of the glabrous surface), but withdrawal still occurred with an even smaller stimulation area (0.3% of the glabrous surface). Using a time-locked, single, 3-ms pulse as a reference, subsequent protective behaviors were recorded using a high-speed camera at 1 kHz to resolve the responses on a millisecond

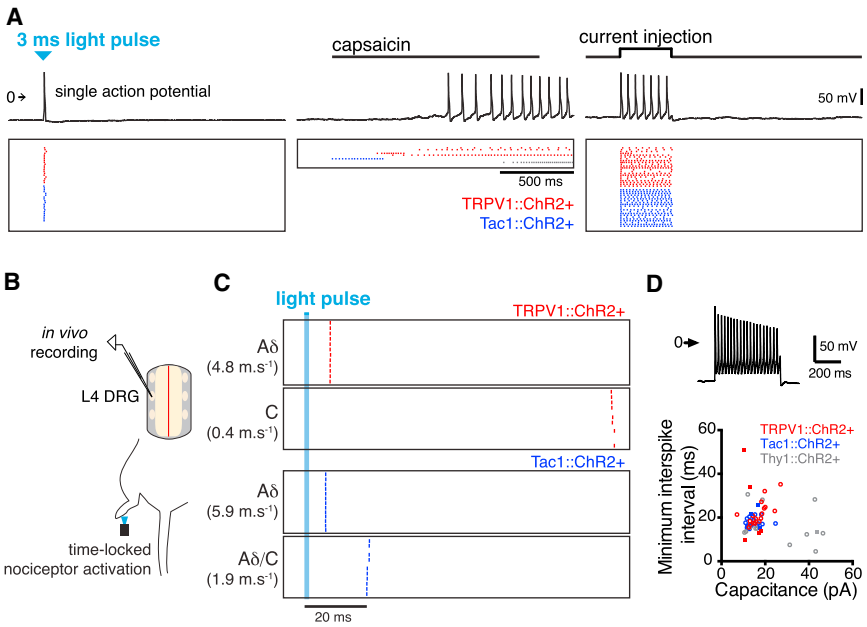

Figure 2. A Single Action Potential Volley Is Sufficient to Drive Nociceptive Behavior

(A) Electrophysiological recordings (top) of a single DRG neuron (TRPV1::ChR2+) shows that one light pulse generates a single action potential, unlike activity evoked by capsaicin (1 μM). Recordings from multiple DRG neurons are plotted as action potential rasters (bottom) evoked by light, capsaicin, or current injection. Each row represents a different neuron.

(B) Optogenetic stimulation in an in vivo cell-attached recording preparation. The plantar surface of the hindpaw was illuminated with a light stimulus, eliciting an action potential that propagated centrally.

(C) Rasters showing the spiking response of four DRG neurons over successive trials. In all cases, the light pulse elicited only single, low-jitter action potentials (0.3%–10.6% of unit interval, 60 trials). Conduction velocities were estimated by a distance between skin and soma of 40 mm.

(D) In vitro whole-cell patch-clamp recordings showing that small-diameter DRG neurons have low maximum firing frequencies. Current was injected in 50-pA increments up to 950 pA to identify the minimum interspike interval. A recording from a TRPV1::ChR2+ neuron injected with 950 pA is shown (top). The minimum interspike interval was plotted against the capacitance (bottom) for 24 TRPV1::ChR2+ neurons, 17 Tac1::ChR2+ neurons, and 21 Thy1::ChR2+ neurons. Thy1::ChR2+ neurons represent a mixed population of small- and large-diameter neurons. Square symbols indicate neurons that also responded to capsaicin (1 μM).

timescale. The temporal and spatial precision and genetic specificity of this approach allowed us to map the fine-grained temporal structure of protective behaviors at the whole-animal level.

First we confirmed that ChR2 expression in TRPV1::ChR2 and Tac1::ChR2 mice indeed matched the profiles for small-diameter C and Aδ nociceptors whose peripheral terminals innervated the epidermis of the skin, and their central axons projected into lamina I–II of the spinal cord dorsal horn (Todd, 2010; Figures 1E and S1A–S1D). These ChR2-expressing dorsal root ganglion (DRG) neurons displayed nociceptor-characteristic high-threshold and wide half-width action potentials in response to both light and current injection (Figures 1F and S1E–S1G; Fang et al., 2005; Petruska et al., 2000). Both mouse lines exhibited normal sensitivity to noxious thermal cutaneous stimuli (Figure S2A). Behavioral responses to light were evoked only by the specific optogenetic activation of afferent fibers (Figures S2B and S2C). TRPV1::ChR2 and Tac1::ChR2 mice therefore represent two complementary but independent DRG nociceptor driver lines and, in the following experiments, produced essentially identical responses.

Whole-cell patch-clamp recordings from cultured DRG neurons from the two mouse lines showed that a single 3-ms pulse of light only ever generated a single action potential, which was time-locked (Figure 2A). The action potential voltage threshold and half-width were identical, whether evoked by optogenetic stimulation or current injection (Figure S1G). DRG neurons negative for ChR2-tdTomato did not display any photocurrents (eight cells).

We confirmed a similar pattern of activation in vivo using loose-patch recordings from targeted DRG neurons in anesthetized mice (Figures 2B and 2C; Bai et al., 2015). Only single action potentials were generated by 3-ms light stimuli to the hindpaw, with very low jitter (0.3%–10.6% of unit interval, 60 trials), which reached the DRG between 6.7 and 100.7 ms after the hindpaw stimulus, indicating activation of both Aδ and C-fibers.

To resolve the precise timing of motor reactions to the time-locked 3-ms light pulse, we recorded evoked behavior at 1 kHz in mice that were "idle" (still and awake; Figure S3) with all paws on the ground (Figure 1B; Movies S1 and S2). The minimal latency for the first observable movement of the hindlimb was 21 and 20 ms for TRPV1::ChR2 and Tac1::ChR2 mice, respectively (Figures 3B and 3D; Figure S4A). The response latencies to first paw withdrawal were distributed in two distinct millisecond timescale populations, around 30 ms and 140 ms. These two different times likely reflect responses to the activation of Aδ or C-fibers, respectively, because there is a high correspondence between these behavioral latencies and the conduction latencies obtained from in vivo loose-patch DRG recordings (Figure 2C). Small-diameter DRG neurons have low maximum firing frequencies and long interspike intervals (Figure 2D), and even under circumstances where a second action potential was evoked by a peripheral stimulus, this would arrive in the CNS too late, after the behavior was completed; thus, fast withdrawal behavior is triggered by arrival of the first set of single action potentials to the spinal cord. The short and the longer latency responses occurred within the same animal in different trials and may reflect either the specific population activated by a particular stimulus or the state of the CNS, which may facilitate or gate different inputs depending on the context of the stimulus.

These electrophysiological, immunohistological, and behavioral experiments indicate that TRPV1-Cre and Tac1-Cre selectively target both Aδ and C-fibers. Although these nociceptive

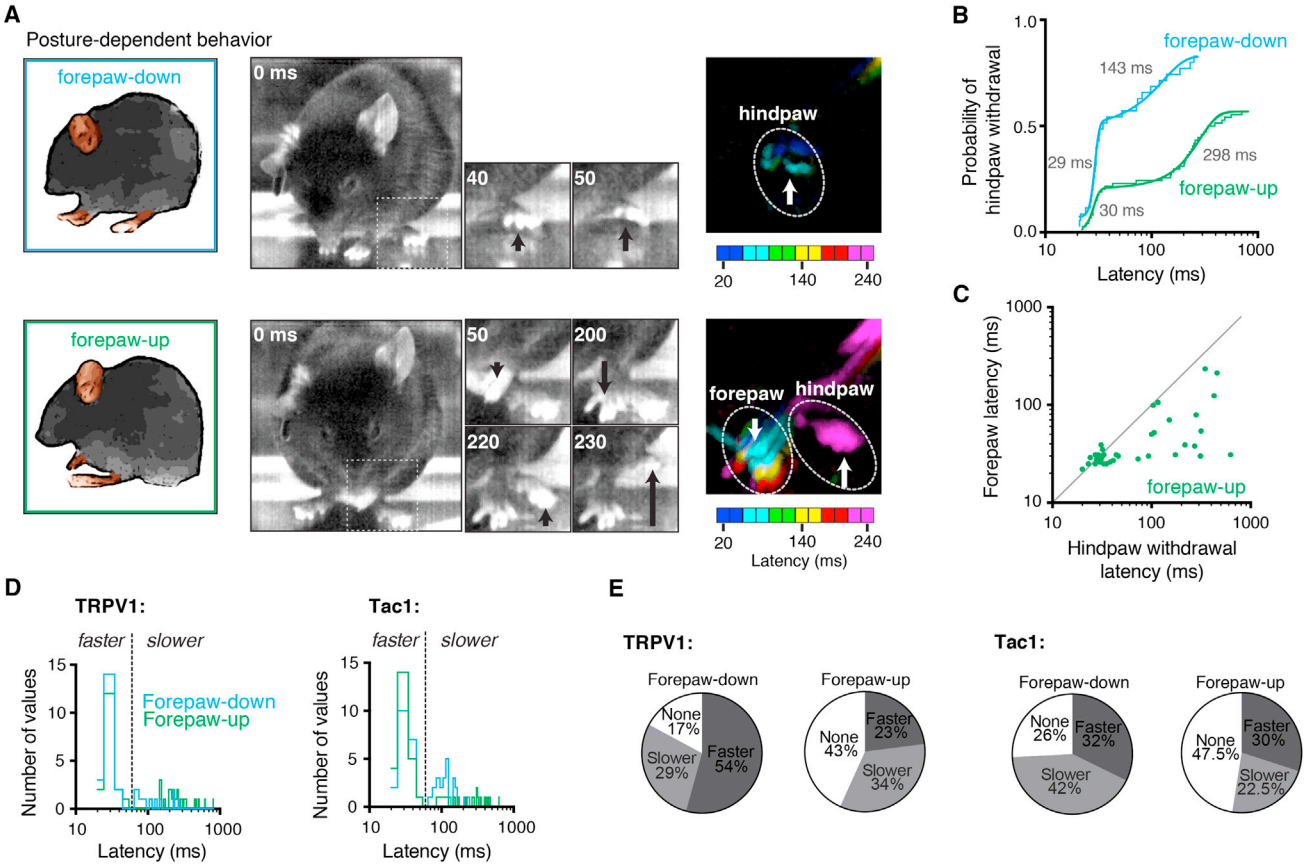

Figure 3. Rapid Nociceptive Behaviors Are Coordinated according to Context

(A) Representative recordings showing posture-dependent nociceptive behaviors recorded from the same animal on the same day. The difference in pixel intensity between frames 20 ms apart illustrates the shift in timings.

(B) Cumulative distributions of hindpaw withdrawal latencies reveal a short response latency in about half the trials and a much slower latency in the others, which is further delayed with forepaw-up. TRPV1::ChR2 is shown for simplicity; see Figure S4 for Tac1::ChR2. Means are shown in gray.

(C) Relative timings for nociceptive hindpaw withdrawal and forepaw extension in response to light in the forepaw-up situation. Most responders are below unity, indicating hindlimb flexion occurring after forepaw extension in the forepaw-up state. TRPV1::ChR2 is shown; see Figure S4 for Tac1::ChR2.

(D) Probability distributions (10-ms bins) for hindpaw withdrawal latency in response to 3-ms optogenetic stimulation in TRPV1::ChR2 and Tac1::ChR2. Cumulative distribution fits (see B and Figure S4A) indicate that the hindpaw withdrawal occurs with two populations. These faster and slower populations were clearly separated at 60 ms (shown by the dashed line), which was used as a cutoff for statistical analysis.

(E) Percentage of trials leading to no response (none) or a fast latency (faster) or slow latency (slower) response, showing that, in the forepaw-up state, the hindpaw withdrawal was either slowed or less likely to occur.

fibers represent a mixture of functionally distinct sensory neuron subtypes, their optogenetic activation is much more selective than that produced by a brief electrical stimulation and without the inevitable activation of low-threshold Aβ fibers, which influence nociceptive pathways (Duan et al., 2014; Melzack and Wall, 1965). The optogenetic strategy allows us to control a genetically defined nociceptive input with single action potential resolution and examine its relationship with the behavioral output at the millisecond timescale.

In wild-type mice, using the same high-speed monitoring of natural stimulus-evoked behavior, we found that thermal stimulation of the hindpaw (100-mW blue light) generated a response with a latency of 1.8 ± 0.4 s (five trials), which is much slower than that activated by optogenetic activation of TRPV1 lineage nociceptors. The delay must reflect the time taken for the skin to heat to a temperature sufficient to activate the nociceptors. Mechanical stimulation (pinprick) of the hindpaw gave a much faster response; 74 ± 12 ms (27 trials), but here it is not possible to dissociate responses evoked by activation of low-threshold from high-threshold mechanoreceptors and the extent of the delay caused by distribution of mechanical forces through the tissue.

Withdrawal Is Not Invariant but Timed According to Context

Mice that were grooming at the time of the stimulus showed substantially reduced withdrawal probabilities (TRPV1::ChR2, 1 of 15 withdrawals; Tac1::ChR2, 11 of 42 withdrawals), suggesting that nociceptive behaviors are actively suppressed in certain contexts (Callahan et al., 2008). In sleeping TRPV1::ChR2 mice

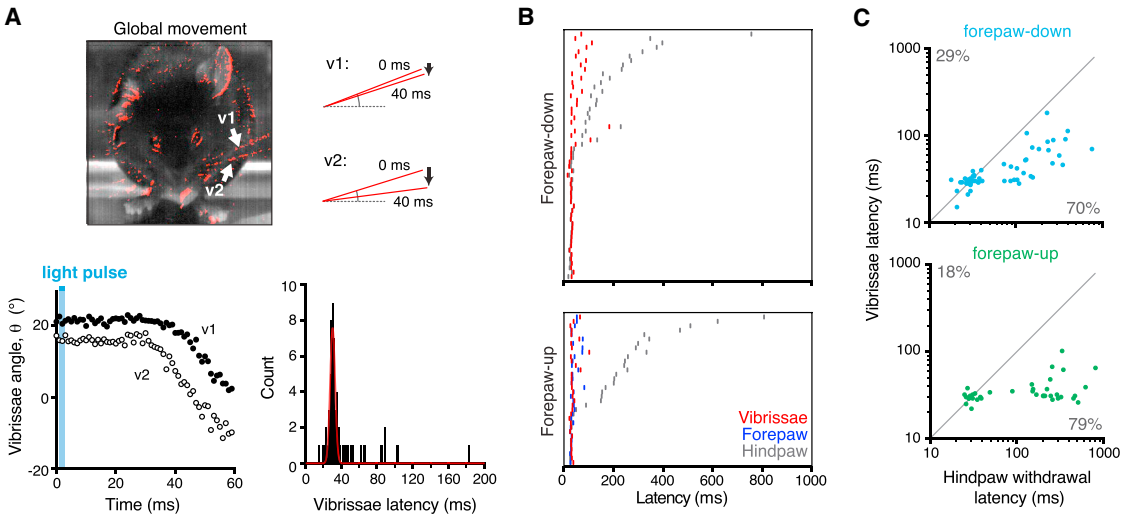

Figure 4. Global Protective Behavioral Responses Occur Simultaneously

(A) Global movements of the whole animal, shown in red, detected by taking the average pixel intensity of ten frames (at 1 kHz) directly before the stimulus and subtracting the pixel intensity of ten consecutive frames beginning 40 ms after stimulus. Downward deflection of vibrissae is clearly resolved (top right, bottom left). The latencies for vibrissa movement fit a Gaussian curve centering on 30 ms (bottom right, 78 recordings).

(B) Rasters for relative latencies for hindpaw withdrawal, forepaw movement, and vibrissa movement showing no change in vibrissae but delayed hindpaw movement in the forepaw-up state.

(C) Relative timings of hindpaw and vibrissa movement in response to light, revealing earlier movement of vibrissae in most cases. TRPV1::ChR2 is shown for simplicity; see Figure S4 for Tac1::ChR2.

(non-REM [rapid eye movement] sleep, determined by electroencephalogram [EEG] recording), flexion was observed in 9 of 20 stimuli, which reflects a reduction in withdrawal probability compared with the awake state, which responded to 33 of 39 stimuli.

High-speed recordings reveal a diversity of responses to the same stimulus (Figure S5) and that the timing of responses was influenced by context. We found that the latency to paw withdrawal was influenced by the posture of the animal (Figure 3; Figures S4A and S4B); hindlimb withdrawal was slower in mice with forepaws raised from the floor ("forepaw-up") compared with mice where all paws were in contact with the floor ("forepaw-down"). Cumulative distributions showed that this effect reflects a delay specifically in the slower-latency putative C-fiber response, which was over 2-fold slower in forepaw-up than in forepaw-down situations (Kolmogorov-Smirnov [K-S] test, $p < 0.0082$). This finding indicates that the timing of the hindlimb flexion withdrawal may be delayed to maintain balance. Consistent with this, in the forepaw-up state, the forelimb moved from its flexed position to an extended position with a fast latency, usually well before hindlimb withdrawal (Figure 3C; Figure S4B; Movie S1). Fast and slow hindpaw behavioral responses occurred in the forepaw-down state with about equal frequency (Figure 3E). The proportion of positive hindpaw responses was overall lower in the forepaw-up compared with the forepaw-down situation (Figure 3E). Therefore, hindlimb withdrawal can be delayed or even, on some occasions, prevented from occurring, perhaps to minimize the summed risk of falling or withdrawal. These findings show that the nociceptive flexion reflex is not hardwired to evoke an invariant withdrawal response at a fixed time but, rather, reflects an integration of diverse influences operating at a sub-second scale.

Local Nociceptor Activation Recruits Responses across the Whole Animal Simultaneously

Single-shot hindpaw optogenetic stimulation did not only result in movements restricted to the limbs but, unexpectedly, also in coordinated movements of the whole animal. The vibrissae showed clear movements, usually well before hindlimb withdrawal (Figures 4 and S4C; Movies S1 and S2). The minimum latencies for vibrissa movement in TRPV1::ChR2 mice (15 ms) and Tac1::ChR2 mice (20 ms) were shorter than hindlimb flexion and indicate recruitment by Aδ afferents. No movement of vibrissae, limbs, head, body, or tail was detected in response to light stimulation in eight control (no ChR2) littermate mice (25 recordings, 400 ms sampled). That a brainstem motor output occurs even before the flexion reflex indicates that the vibrissae are part of a global protective system to very rapidly identify the spatial source of danger.

High-speed recordings show that global responses also occur with a natural noxious mechanical stimulus (pinprick). The latency for global responses in this situation occurred at 37 ± 9 ms, whereas the stimulated hind paw responded at 104 ± 26 ms (six responses). Both low-threshold and high-threshold mechanoreceptors are activated by this stimulus. However, using optogenetics, we reveal that nociceptors alone are sufficient to drive millisecond-timescale spinal segmental responses as well as ones initiated in the brain and that the latter generally occur before the former.

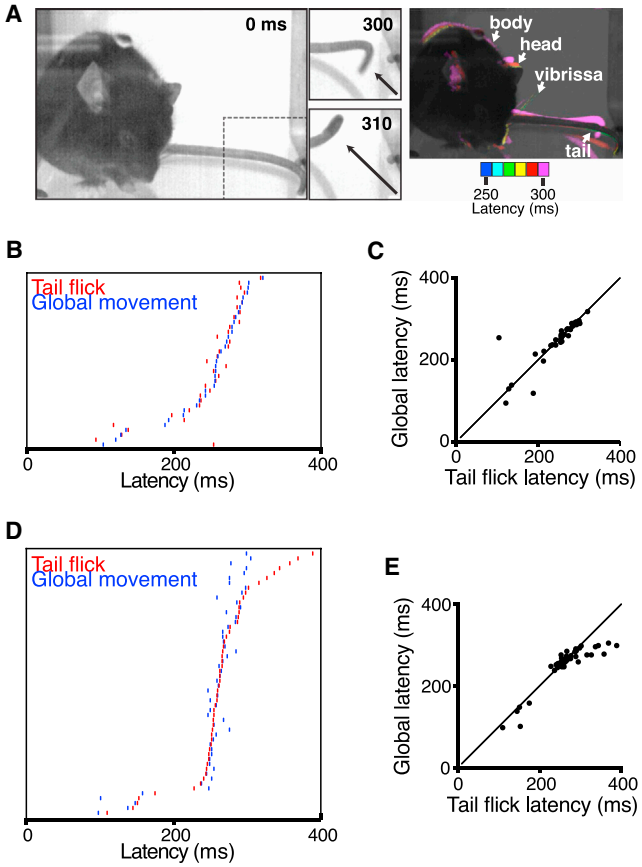

Figure 5. Time-Resolved Tail Flick Reflex

(A) A 3-ms pulse of light to the distal tail tip drove coincident local tail movement and global protective behaviors. The difference in pixel intensity at 10-ms intervals illustrating relative latencies is shown on the right for a TRPV1::ChR2 mouse as an example.

(B) Rasters showing similar latencies for tail flick and global movements (vibrissae, head, and body) in TRPV1::ChR2 mice.

(C) Relative timings of TRPV1::ChR2 tail flick and global movements in response optogenetic stimulation (35 recordings). Slope = 0.99, Pearson's r = 0.85.

(D) Raster plot showing coincident timings of optogenetically evoked tail flick and global movements (vibrissae, head, and body) in Tac1::ChR2 mice.

(E) Relative timings of Tac1::ChR2 tail flick and global movements in response optogenetic stimulation (n = 54). Slope = 0.96, Pearson's r = 0.89.

Tail flick is another spinal withdrawal reflex, enabling escape of this body part from potentially injurious stimuli. Single-shot optogenetic activation of the tail flick reflex initiated a localized tail withdrawal response, which was concurrent with widespread movements of the vibrissae, head, body, and limbs (Figure 5; Movie S3). Absolute latencies for tail responses were longer than for stimulation of the hindpaw, with a minimum latency of 104 ms (TRPV1, 35 recordings from 8 mice) and 110 ms (Tac1, 54 recordings from 8 mice) and means of 247 ± 9 ms and 263 ± 7 ms, respectively. This provided an extended time window in which to resolve distinct global behavioral latencies. These behaviors are likely, given the latency, to be driven mainly by C-fiber input, unlike the hindpaw, where we observed short

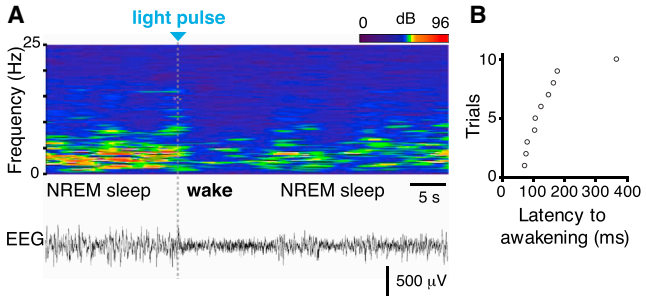

Figure 6. Minimal Nociceptor Activation Causes Sub-second Awakening

(A) Latency to awakening in response to optogenetic stimulation applied to TRPV1::ChR2 mice during non-rapid eye movement (NREM) sleep detected by EEG/electromyogram (EMG) analysis. Top, heatmap representation of the EEG power spectrogram (0–25 Hz). Bottom, corresponding EEG trace. The gray bar represents the 3-ms stimulation. Note that the animal woke with a very short latency and resumed sleep quickly.

(B) Latency to awakening from NREM sleep after stimulation in ten trials.

and long latency responses, which may reflect different sensory innervation in these tissues. Although hindlimb stimulation invariably generated short-latency, Aδ-evoked general body (whisker) movements, the long latency of the general body movements evoked in response to tail stimulation indicates that C-fibers can also access distributed alerting responses. Although, like hindlimb withdrawal, the tail flick was considered to represent only a localized spinal reflex (Irwin et al., 1951), our data indicate that nociceptor activation in the tail evokes behaviors that are not limited to the spinal cord but extend globally to produce coordinated widespread sub-second protective responses.

Sub-second Awakening on Minimal Nociceptor Activation

Cortical EEG recordings during brief 3-ms optogenetic stimulation in sleeping mice showed that the stimulation provoked the mice to wake with a latency consistent with C-fiber activation (Figure 6). Input from those few nociceptors innervating a small area of hindpaw skin has, therefore, widespread consequences in the CNS that include terminating sleep within a fraction of a second (156 ± 29 ms, n = 9)—an order of magnitude faster than with an innocuous acoustic tone (Kaur et al., 2013). This reveals that the sleep-to-wake transition can occur very rapidly in response to danger; cortical activity can be changed within a fraction of a second by a single action potential volley initiated at the skin in nociceptors.

DISCUSSION

Primary afferent nociceptors are genetically and functionally heterogeneous, allowing for discriminative detection of many somatic sensory modalities, intensities, and timings, including noxious thermal, mechanical, and chemical stimuli. In an experimental setting, the controlled application of a thermal, mechanical, or chemical stimulus is designed to mimic naturalistic activation of cutaneous afferents in a real-life setting and has been essential in studying the neural underpinnings of sensory

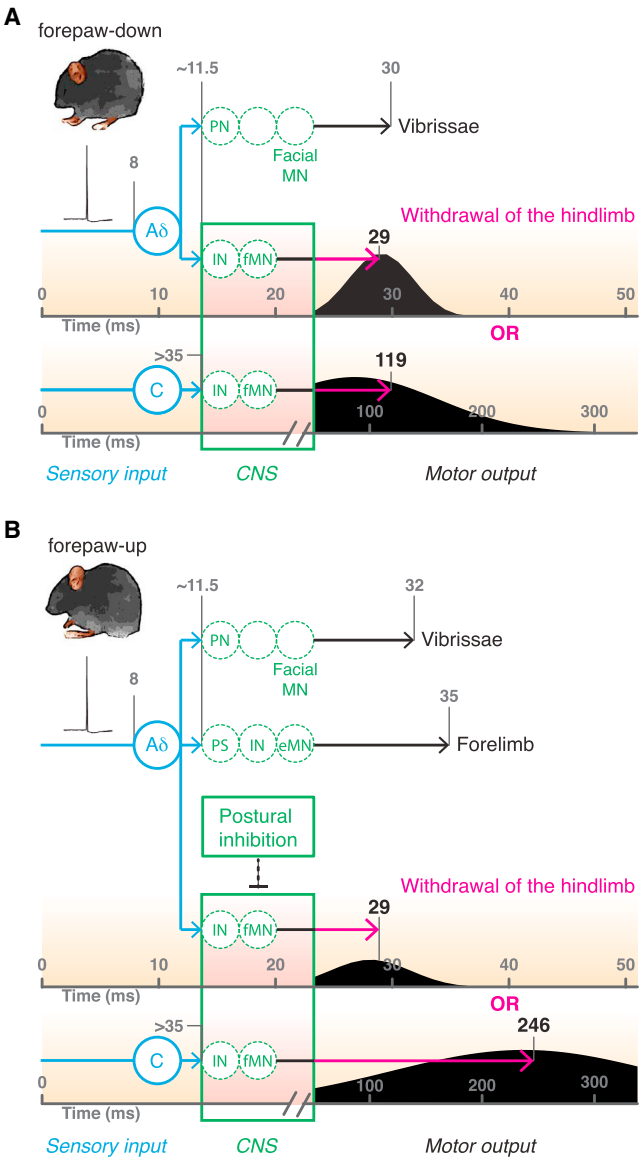

Figure 7. Model of Context-Dependent Flexion Reflex Gating

Brief optogenetic activation of hindpaw nociceptors (in blue) generates a single action potential volley in Aδ and C-fibers that travels at ~5 m/s and <1.5 m/s, respectively, to reach the spinal cord at ~11.5 and >35 ms.

(A) In the forepaw-down state, the afferent input drives spinal interneurons (IN) to activate flexor motor neurons (fMN) in the ventral horn, leading to hindlimb flexion. Normalized probability distributions (black curves) were calculated from the first derivate of fits in Figure 3B with median latency values. Aδ nociceptors simultaneously activate projection neurons to recruit activity in supraspinal motor neurons that control vibrissa movement.

(B) In the forepaw-up state, the Aδ response is unchanged in time, although reduced in frequency, but the C-fiber response is delayed or absent; in this postural position, hindlimb flexor motor neurons are tonically inhibited.

Noc, nociceptor; PN, projection neuron; IN, interneuron; PS, propriospinal neuron connecting lumbar and cervical circuits; MN, motor neuron, where fMN is flexor and eMN is extensor. Calculations were based on distance between the glabrous skin of the hindpaw to DRG, ~40 mm; distance between the DRG and spinal cord, ~10 mm; synaptic delay, ~1.5 ms; and MN conduction, neuromuscular junction delay, and excitation contraction coupling, ~7 ms.

processing. In spite of this, the fundamental principles underlying nociceptor coding remain unclear; for example, the extent to which polymodal nociceptors contribute to coding (Prescott et al., 2014). One problem is that any naturalistic stimulus, however brief, will necessarily activate multiple subpopulations of nociceptors at different times, and, in most cases, low-threshold afferents also, making it difficult to define the particular consequences of specific inputs from one class of neuron. Studying some of the fundamental properties of nociceptors and the behavioral responses they evoke in vivo requires greater specificity and temporal control than that afforded by such naturalistic stimuli. These stimuli are typically applied at a timescale that is slower than the timescale for the nervous system to respond (millisecond). Indeed, high-threshold nociceptors do not fire until the stimulus applied to the skin tissue has reached the activation threshold of transducers on their peripheral terminals by changing the temperature of the skin, transferring force through the skin or the diffusion of chemicals to the receptors.

We used optogenetic stimulation in this study as an alternative strategy to naturalistic stimuli to both obtain the genetic specificity of the class of afferent activated and to give us high temporal single action potential resolution. This approach, by bypassing delays because of sensory transduction mechanisms, allows direct study, in the millisecond range, of the central consequences of defined inputs. Our data show that optogenetic stimulation provides unique advantages for understanding the temporal relationship between a specific nociceptor input and its output that are not possible with naturalistic stimulation. Precise control of which afferent is stimulated and when is obviously artificial in its nature; normally, such a limited input is unlikely to occur, but it does enable important aspects of sensory responses to be experimentally measured. Our data showing that pinprick-like optogenetic stimuli elicit global responses indicate that the nature of the response evoked by the optogenetic stimulation does not differ qualitatively from that produced by naturalistic stimuli.

In the present study, we combine high spatiotemporal resolution and minimal genetically specific input to examine fast protective stimulus-response relationships across the whole animal in freely behaving mice at a millisecond timescale. Nociceptors innervating skin were genetically targeted and optically stimulated using a single short pulse of light so that the timings of behavioral responses could be resolved with a high-speed camera at 1 kHz. Combining optogenetics with millisecond timescale sampling of global behavior reveals behavioral features that otherwise could not have been observed. This strategy has provided insight into the operation of the CNS related to the initiating alerting responses to danger and the coordinating of body movement to minimize potential harm (Figure 7) but also relates to more general aspects of CNS organization at a sub-second scale.

Rodents can be trained to report on single action potentials in a few hundred neurons in the barrel cortex (Huber et al., 2008). Such associative learning can also be achieved with a train of action potentials in a single neuron in the motor cortex and somatosensory cortex (Brecht et al., 2004; Houweling and Brecht, 2008). In larval zebrafish, a single action potential in a single trigeminal neuron is sufficient to drive escape behavior

(Douglass et al., 2008). We find that initiation of a single action potential volley in mammalian primary sensory neurons is also sufficient to elicit robust innate protective behaviors, in agreement with the recent findings of others (Arcourt et al., 2017). These authors measured the resultant local segmental responses at 240 frames per second. Here we develop this approach further and exploit the time-locked single action potential input to map the precise temporal structure of the resultant fast behavior at the millisecond timescale and the whole-animal level.

Over a century ago, Sherrington described the nociceptive flexion-reflex of the limb and its properties in decerebrate and spinal cat preparations; noxious stimulation of the hindlimb simultaneously activates flexor muscles and inhibits extensor muscles to withdraw the limb from the stimulus (Sherrington, 1906, 1910). Forelimb reflex movements accessory to this protective reflex were also observed in these preparations (Sherrington, 1906, 1910). Here we show that in freely behaving mice, movements in the vibrissae, head, body, and forelimbs occur simultaneously with movement of the hindlimb. Thus, information arriving in one highly spatially restricted part of the dorsal horn of the spinal cord by single action potentials in a small number of sensory fibers appears to be rapidly distributed across many different parts of the CNS to initiate multiple rapid and diverse movements. This response includes the initiation of exploratory movements by the vibrissa sensory system, which has important roles in sampling the environment (Moore, 2004) and coordinate protection of the animal. Activation of vibrissa movement was particularly highly time-locked with the jitter expected of a polysynaptic circuit. The nociceptor input was also sufficient to terminate sleep within a fraction of a second. This rapid transition from sleep to wake states promotes transient arousal, potentially to prepare to flee from the stimulus source. This illustrates how widespread the circuits are that can be recruited by minimal nociceptive input.

We observe that certain behavioral responses are suppressed or delayed, depending on the ongoing state of the animal, as set by body position and activities like grooming. These findings suggest that information about body state is distributed to determine the nature and timing of any response elicited at a particular time from a particular location. How circuits run extended programs from a single action potential input and how and where interactive postural and activity gating operates now need to be established, including where nociceptive information is stored in the CNS until movement is permitted by the relief of any gating long after the input is over.

Taken together, our data show that the system operates like a tripwire so that minimal input to the central nervous system triggers widespread but coordinated and interactive neural programs that, when activated, become independent of any need for further afferent input. This set of widely distributed interacting circuits is far more complex than the prototypic primary nociceptive protective reflex response: a short polysynaptic chain of excitatory interneurons to ipsilateral flexor motor neurons and inhibitory interneurons to extensor motor neurons in the same spinal cord segment. The resolution afforded by combining optogenetics with global millisecond behavioral response mapping of awake behaving animals has revealed an unsuspected complexity of even the simplest of nervous system stimulus-response relationships, one that now needs to be reconciled with growing insights into the dynamic network states present in neural microcircuitry (Markram et al., 2015). We reveal that a single input in a very limited skin area drives multiple parallel innate programs distributed throughout the spinal cord, brain stem, and cortex that alert the animal to and protect it from danger in a dynamic manner that reflects its current state, reinforcing the presence in the CNS of selectable, complex, and diverse sub-second behavioral responses (Wiltschko et al., 2015). The identity of the circuits that guide these dynamic sub-second responses and their influence on the experience of pain can now be investigated.

EXPERIMENTAL PROCEDURES

Further details and an outline of resources used in this work can be found in the Supplemental Experimental Procedures.

Mice

Targeted expression of ChR2-tdTomato in nociceptive primary afferents was achieved by breeding heterozygous Rosa-CAG-LSL-hChR2(H134R)-tdTomato-WPRE (Ai27D) mice (Madisen et al., 2012) with mice with Cre recombinase inserted downstream of the *Trpv1* (Cavanaugh et al., 2011) or *Tac1* genes (Harris et al., 2014). The background strain was C57BL/6j. Resultant mice were heterozygous for both transgenes and were housed with control littermates. Mice were given ad libitum access to food and water and were housed in 22°C ± 1°C, 50% relative humidity, and a 12 hr light:12 hr dark cycle. Adult (2–6 months old) mice were used in the experiments. Male and female mice were pooled by genotype to limit the number of animals used.

All experiments were carried out at Boston Children's Hospital and Harvard Medical School and were conducted according to institutional animal care and safety guidelines and with Institutional Animal Care and Use Committee (IACUC) approval.

Behavioral Studies

Experiments were conducted in a quiet room at 22°C ± 1°C with 50% relative humidity. Animals were acclimatized to the behavioral testing apparatus during three habituation sessions in advance of starting the experiment. The behavioral tester was blinded, and randomization was achieved through a breeding strategy where mice were separated based on their sex during weaning.

In Vivo Optogenetics

Mice were placed on a borosilicate glass (1.1 mm thick) platform in 7.5 × 7.5 × 15 cm chambers and acclimatized for at least 1 hr. A requirement was that the mice were in a calm and awake idle state and not grooming or exploring so that there was minimal movement before optogenetic stimulation, increasing the signal-to-noise ratio. "Non-idle" states were identified as a body posture that was lowered to the floor; because these mice were likely not awake, they were not used (Figure S3). A 473-nm diode pumped solid state (DPSS) laser (100 mW, LaserGlow) coupled to a multimode optical fiber (400-μm core diameter, 1-m length, Thorlabs) was used in all behavioral experiments. A computer-controlled pulse generator (OPTG-4, Doric) was used to supply TTL signals to the laser driver. Average power density was estimated by sampling 400 pulses over 20 s using a PS19 optical power meter (Coherent). The optical fiber tip was positioned below the left hindpaw during optogenetic stimulation (3 ms at 47 mW/mm^2). This was consistently applied to the center of the lateral plantar glabrous surface to minimize any differences in innervation density. A 3-ms pulse duration was selected to accurately resolve the relatively short response times. Behavior was sampled at 1,000 frames per second using an acA2040-180kmNIR Cameralink complementary metal-oxide-semiconductor (CMOS) camera (Basler) with an 8-mm lens and set at 500 × 350 pixels under normal ambient lighting (800-μs exposure time). Light saturation

was reduced by a yellow-orange lens filter. Acquisition was carried out using LabVIEW on a computer with excess buffer capacity to ensure that all frames were successfully retained. An oscilloscope was used to confirm the frame rate. An Edgertronic high-speed camera was also used. All experiments used at least two independent litters and were duplicated. Hindpaw, forelimb, vibrissa, head, and body latencies were determined manually frame by frame. Littermate controls without Cre recombinase or without ChR2 never reacted to a 10-ms blue light pulse (3 trials for 15 mice). TRPV1::ChR2 and Tac1::ChR2 mice did not respond to an equivalent off-spectrum pulse of light (594 nm, three trials in seven mice each for TRPV1::ChR2 and Tac1::ChR2).

Statistical Methods

Pooled data are given as the mean ± SEM unless specified otherwise. Two-tailed unpaired Student's t test was used to compare a single measurement between two groups. Nonparametric ANOVA was used for multiple comparisons of statistical significance. In all tests, $p < 0.05$ was considered significant. The glabrous hindpaw surface was 56 ± 1 mm^2 (both paws in ten mice). The minimal latency for the first observable movement of the hindlimb was 21 ms for TRPV1::ChR2 (36 trials, 13 mice) and 20 ms for Tac1::ChR2 mice (63 trials, 10 mice). Kolmogorov-Smirnov test was used to compare cumulative distributions that were separated into fast and slow populations using a threshold of 60 ms (Figure 3). The response latencies to the first paw movement are shown as means of 29 ± 1 and 143 ± 24 ms (from 19 and 10 responses, respectively) for TRPV1::ChR2 mice and 32 ± 2 ms or 129 ± 17 ms (from 20 and 26 responses) for Tac1::ChR2 mice.

SUPPLEMENTAL INFORMATION

Supplemental Information includes Supplemental Experimental Procedures, five figures, and three movies and can be found with this article online at http://dx.doi.org/10.1016/j.celrep.2017.06.024.

AUTHOR CONTRIBUTIONS

Conceptualization, L.E.B. and C.J.W.; Methodology, L.E.B. and C.J.W.; Investigation, L.E.B., A.L., B.P.L., A.G., C.W., C.A., and M.C.; Formal Analysis, L.E.B., A.L., B.P.L., and C.A.; Resources, L.E.B, D.P.R., and F.M.; Validation, A.G. and C.W.; Writing – Original Draft, L.E.B. and C.J.W.; Writing – Review & Editing, L.E.B., A.L., B.P.L., M.C., F.M., D.D.G., and C.J.W.; Visualization, L.E.B., A.L., and C.J.W.; Funding Acquisition, L.E.B. and C.J.W.; Supervision, L.E.B. and C.J.W.

ACKNOWLEDGMENTS

This work was supported by NIH RO1DE022912, R01NS038253, and R37NS039518 (to C.J.W.), R35NS97344 (to D.D.G), and F32NS095631 (to B.P.L.); a Marie Curie Actions Fellowship from the European Commission (329202); and a Sir Henry Dale Fellowship jointly funded by the Wellcome Trust and the Royal Society (109372/Z/15/Z) (to L.E.B.).

Received: January 4, 2017
Revised: March 3, 2017
Accepted: June 6, 2017
Published: July 5, 2017

REFERENCES

Arcourt, A., Gorham, L., Dhandapani, R., Prato, V., Taberner, F.J., Wende, H., Gangadharan, V., Birchmeier, C., Heppenstall, P.A., and Lechner, S.G. (2017). Touch Receptor-Derived Sensory Information Alleviates Acute Pain Signaling and Fine-Tunes Nociceptive Reflex Coordination. Neuron *93*, 179–193.

Bai, L., Lehnert, B.P., Liu, J., Neubarth, N.L., Dickendesher, T.L., Nwe, P.H., Cassidy, C., Woodbury, C.J., and Ginty, D.D. (2015). Genetic Identification of an Expansive Mechanoreceptor Sensitive to Skin Stroking. Cell *163*, 1783–1795.

Basbaum, A.I., Bautista, D.M., Scherrer, G., and Julius, D. (2009). Cellular and molecular mechanisms of pain. Cell *139*, 267–284.

Brecht, M., Schneider, M., Sakmann, B., and Margrie, T.W. (2004). Whisker movements evoked by stimulation of single pyramidal cells in rat motor cortex. Nature *427*, 704–710.

Callahan, B.L., Gil, A.S., Levesque, A., and Mogil, J.S. (2008). Modulation of mechanical and thermal nociceptive sensitivity in the laboratory mouse by behavioral state. J. Pain *9*, 174–184.

Cavanaugh, D.J., Chesler, A.T., Jackson, A.C., Sigal, Y.M., Yamanaka, H., Grant, R., O'Donnell, D., Nicoll, R.A., Shah, N.M., Julius, D., and Basbaum, A.I. (2011). Trpv1 reporter mice reveal highly restricted brain distribution and functional expression in arteriolar smooth muscle cells. J. Neurosci. *31*, 5067–5077.

Clarke, R.W., and Harris, J. (2004). The organization of motor responses to noxious stimuli. Brain Res. Brain Res. Rev. *46*, 163–172.

Daou, I., Tuttle, A.H., Longo, G., Wieskopf, J.S., Bonin, R.P., Ase, A.R., Wood, J.N., De Koninck, Y., Ribeiro-da-Silva, A., Mogil, J.S., and Séguéla, P. (2013). Remote optogenetic activation and sensitization of pain pathways in freely moving mice. J. Neurosci. *33*, 18631–18640.

Douglass, A.D., Kraves, S., Deisseroth, K., Schier, A.F., and Engert, F. (2008). Escape behavior elicited by single, channelrhodopsin-2-evoked spikes in zebrafish somatosensory neurons. Curr. Biol. *18*, 1133–1137.

Duan, B., Cheng, L., Bourane, S., Britz, O., Padilla, C., Garcia-Campmany, L., Krashes, M., Knowlton, W., Velasquez, T., Ren, X., et al. (2014). Identification of spinal circuits transmitting and gating mechanical pain. Cell *159*, 1417–1432.

Fang, X., McMullan, S., Lawson, S.N., and Djouhri, L. (2005). Electrophysiological differences between nociceptive and non-nociceptive dorsal root ganglion neurones in the rat in vivo. J. Physiol. *565*, 927–943.

Harris, J.A., Hirokawa, K.E., Sorensen, S.A., Gu, H., Mills, M., Ng, L.L., Bohn, P., Mortrud, M., Ouellette, B., Kidney, J., et al. (2014). Anatomical characterization of Cre driver mice for neural circuit mapping and manipulation. Front. Neural Circuits *8*, 76.

Houweling, A.R., and Brecht, M. (2008). Behavioural report of single neuron stimulation in somatosensory cortex. Nature *451*, 65–68.

Huber, D., Petreanu, L., Ghitani, N., Ranade, S., Hromádka, T., Mainen, Z., and Svoboda, K. (2008). Sparse optical microstimulation in barrel cortex drives learned behaviour in freely moving mice. Nature *451*, 61–64.

Irwin, S., Houde, R.W., Bennett, D.R., Hendershot, L.C., and Seevers, M.H. (1951). The effects of morphine methadone and meperidine on some reflex responses of spinal animals to nociceptive stimulation. J. Pharmacol. Exp. Ther. *101*, 132–143.

Iyer, S.M., Montgomery, K.L., Towne, C., Lee, S.Y., Ramakrishnan, C., Deisseroth, K., and Delp, S.L. (2014). Virally mediated optogenetic excitation and inhibition of pain in freely moving nontransgenic mice. Nat. Biotechnol. *32*, 274–278.

Julius, D. (2013). TRP channels and pain. Annu. Rev. Cell Dev. Biol. *29*, 355–384.

Kaur, S., Pedersen, N.P., Yokota, S., Hur, E.E., Fuller, P.M., Lazarus, M., Chamberlin, N.L., and Saper, C.B. (2013). Glutamatergic signaling from the parabrachial nucleus plays a critical role in hypercapnic arousal. J. Neurosci. *33*, 7627–7640.

Madisen, L., Mao, T., Koch, H., Zhuo, J.M., Berenyi, A., Fujisawa, S., Hsu, Y.W., Garcia, A.J., 3rd, Gu, X., Zanella, S., et al. (2012). A toolbox of Cre-dependent optogenetic transgenic mice for light-induced activation and silencing. Nat. Neurosci. *15*, 793–802.

Markram, H., Muller, E., Ramaswamy, S., Reimann, M.W., Abdellah, M., Sanchez, C.A., Ailamaki, A., Alonso-Nanclares, L., Antille, N., Arsever, S., et al. (2015). Reconstruction and Simulation of Neocortical Microcircuitry. Cell *163*, 456–492.

Melzack, R., and Wall, P.D. (1965). Pain mechanisms: a new theory. Science *150*, 971–979.

Moore, C.I. (2004). Frequency-dependent processing in the vibrissa sensory system. J. Neurophysiol. *91*, 2390–2399.

Petruska, J.C., Napaporn, J., Johnson, R.D., Gu, J.G., and Cooper, B.Y. (2000). Subclassified acutely dissociated cells of rat DRG: histochemistry and patterns of capsaicin-, proton-, and ATP-activated currents. J. Neurophysiol. *84*, 2365–2379.

Prescott, S.A., Ma, Q., and De Koninck, Y. (2014). Normal and abnormal coding of somatosensory stimuli causing pain. Nat. Neurosci. *17*, 183–191.

Schouenborg, J., and Kalliomäki, J. (1990). Functional organization of the nociceptive withdrawal reflexes. I. Activation of hindlimb muscles in the rat. Exp. Brain Res. *83*, 67–78.

Schouenborg, J., and Weng, H.R. (1994). Sensorimotor transformation in a spinal motor system. Exp. Brain Res. *100*, 170–174.

Sherrington, C.S.S. (1906). Integrative action of the nervous system (New Haven: Yale U.P).

Sherrington, C.S. (1910). Flexion-reflex of the limb, crossed extension-reflex, and reflex stepping and standing. J. Physiol. *40*, 28–121.

Todd, A.J. (2010). Neuronal circuitry for pain processing in the dorsal horn. Nat. Rev. Neurosci. *11*, 823–836.

Wiltschko, A.B., Johnson, M.J., Iurilli, G., Peterson, R.E., Katon, J.M., Pashkovski, S.L., Abraira, V.E., Adams, R.P., and Datta, S.R. (2015). Mapping Sub-Second Structure in Mouse Behavior. Neuron *88*, 1121–1135.

Woolf, C.J. (1983). Evidence for a central component of post-injury pain hypersensitivity. Nature *306*, 686–688.